

Substantial Improvement of Pyridine-Carbene Iridium Water Oxidation Catalysts by a Simple Methyl-to-Octyl Substitution

Ilaria Corbucci,[†] Ana Petronilho,[‡] Helge Müller-Bunz,[‡] Luca Rocchigiani,[†] Martin Albrecht,^{*,‡} and Alceo Macchioni^{*,†}

[†]Department of Chemistry, Biology and Biotechnology, University of Perugia, Via Elce di Sotto, 8, I-06123, Perugia, Italy [‡]School of Chemistry and Chemical Biology, University College Dublin, Belfield, Dublin 4, Ireland

Supporting Information Placeholder

ABSTRACT: The substitution of a methyl to an octyl group in the ancillary triazolylidene ligand—an apparently simple variation—induces a more than 10-fold increase of activity of the corresponding iridium complex in water oxidation catalysis when using cerium(IV) as sacrificial oxidant. Detailed NMR studies suggest that various different molecular species form, all bearing the intact triazolylidene ligand. The octyl substituent is essential for inducing the association of the iridium species thus generating extraordinarily active multi-metallic catalytic sites. Their accessibility and steady state concentration is critically dependent on the type of sacrificial oxidant and specifically on the CAN vs catalyst ratio. **KEYWORDS:** Water Oxidation; Iridium; Homogeneous Catalysis; Mesoionic Carbenes; Aggregation.

Water oxidation (WO) to molecular oxygen has been recognized as the essential process for producing reductive equivalents for the storage of solar fuels by means of artificial photosynthesis.^{1a-f} In addition to its endergonic thermodynamics, WO is complicated kinetically because of the multi-proton/multielectron transfers involved. Therefore WO requires a competent catalyst (C) that offers an energetically more feasible reaction pathway. Several WOCs have been reported so far,^{2a-f,3} including molecular systems which are receiving much attention since their performance can potentially be tailored and optimized by an appropriate selection of the ancillary ligands.⁴ For example, Sun, Llobet and coworkers demonstrated that changing an ancillary ligand in a ruthenium complex from 4-picoline to isoquinoline induces a remarkable 10-fold increase of activity.⁵

Organometallic iridium-based WOCs constitute a class of compounds that is particularly suitable for exploring ligand tailoring.⁶ Based on Bernhard's pioneering work using $[\text{Ir}(\text{ppy})_2(\text{H}_2\text{O})_2]^+$ (ppy = 2-phenylpyridine),⁷ compounds

of formula $[\text{Cp}^*\text{IrL}^1\text{L}^2\text{L}^3]$ (Cp* = pentamethylcyclopentadienyl C_5Me_5^-) emerged as highly active WOCs.^{8a-j} The ancillary ligands L in these complexes play a critical role in modulating the catalytic performance and also in determining the nature of the active species, altering *e.g.* the tendency of the Cp* ligand to undergo oxidative transformations.^{9a-c} Such Cp* oxidation has been suggested to be essential for accessing the true catalytically active species,^{10a-b} thus emphasizing the relevance of ancillary ligands that bind robustly to iridium in order to maintain a homogeneously operating and molecularly well-defined catalyst, with^{11a-b} or without^{12a-b} fragments of the modified Cp* ligand.

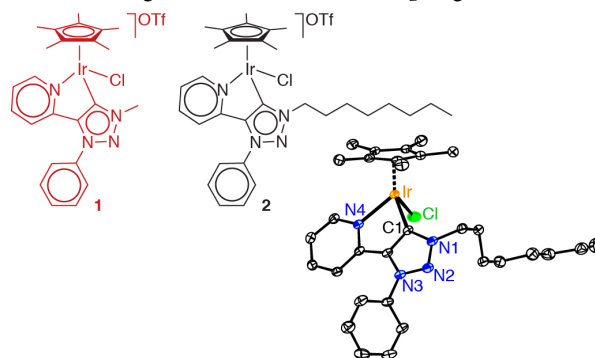


Figure 1. Sketch of iridium WOC precursors **1** and **2** bearing a mesoionic N,C-bidentate carbene ligand, and ORTEP plot (50% probability ellipsoids) of complex **2**.

We have recently reported highly efficient iridium WOCs containing mesoionic C,C- and N,C-bidentate triazole-derived carbene ligands as ancillary ligands.^{13a-c} Detailed kinetic and mechanistic investigations strongly support a homogeneous mode of action of the most active species, hence warranting further work on ligand tailoring to improve catalytic activity. Herein we report the synthesis of new WOCs based on related mesoionic N,C-bidentate triazolylidene^{14a-d} ligands (Figure 1) and provide evidence that a peripheral modification of an apparently innocent methyl group to an

octyl group causes an enormous enhancement of catalytic WO activity when cerium ammonium nitrate (CAN, $(\text{NH}_4)_2[\text{Ce}(\text{NO}_3)_6]$) is used as sacrificial oxidant, whereas effects are only marginal with NaIO_4 as terminal oxidant.^{15a-b}

Complexes **1** and **2** contain a methyl and an octyl group, respectively, as the triazolylidene *N*-substituent. These complexes were synthesized in three steps from phenyl azide and 2-ethynylpyridine. Base-catalyzed [3+2] cycloaddition afforded the 1,5-substituted triazole.¹⁶ Subsequent alkylation with MeI yielded an easily separable mixture of mono- and dimethylated products while bromooctane addition occurred selectively at the triazole nitrogen. Finally, metalation of the triazolium salts was accomplished via in-situ generation of a silver triazolylidene intermediate followed by transmetalation with $[\text{IrCp}^*\text{Cl}_2]_2$.¹³

The solid state structure of **2** was determined by X-ray diffraction analysis (Figure 1).¹⁷ Multinuclear and multidimensional NMR experiments allowed the complete assignment of all resonances and revealed high similarity of **1** and **2**. For instance, the carbene carbon nucleus resonates at 157.0 ppm and 156.2 ppm in **1** and **2**, respectively. Likewise, the electrochemical behavior is not significantly altered and no oxidation occurs below +1.6 V (*vs* NHE).

Complexes **1** and **2** were evaluated as WOCs using CAN or NaIO_4 as sacrificial oxidant (SO). Catalytic activity was monitored by UV-Vis spectroscopy (consumption of CAN), by manometry, and by Clark electrode measurements (O_2 evolution). Representative data including TOF and TON values at different concentrations of SO and iridium complex are summarized in Table 1.¹⁷ In terms of activity, complex **1** ($\text{TOF}_{\text{max}} = 16 \text{ min}^{-1}$ and 19 min^{-1} with CAN and NaIO_4 , respectively) compares well with the most active iridium WOCs known to date,^{2b-c} and the rate does not depend significantly on the catalysts concentration nor on the nature and concentration of the sacrificial oxidant. A similar behavior was noted for the activity of **2** with NaIO_4 as sacrificial oxidant, although rates ($\text{TOF}_{\text{max}} = 7 \text{ min}^{-1}$) were slightly lower than for **1**. A drastically different behavior was observed for water oxidation with **2** driven by CAN. The activity strongly depends on the concentrations of catalyst and of CAN and reaches much higher rates, $\text{TOF}_{\text{max}} = 116 \text{ min}^{-1}$, which are up to one order of magnitude higher than those of **1** and other best-performing iridium-based WOCs (Figure 2).¹⁷ In order to rationalize the remarkably high and CAN-dependent activity of complex **2**, a series of comparative catalytic experiments were carried out for **1** and **2** under identical conditions. These experiments reveal that both complexes **1** and **2** induce identical initial oxygen evolution rates (e.g. $\text{TOF}_{\text{ini}} = 10 \text{ min}^{-1}$ in Figure 2). At a specific time, t_B = bifurcation time, the activity of complex **2** increases substantially, while complex **1** continues to produce oxygen at a constant rate identical to TOF_{ini} (inset Figure 2).

Table 1. Selected catalytic activity data of WOC precursors **1 and **2**.**^a

Entry	[Cat] / μM	SO	UV-Vis		manometry		Clark
			TOF	TON	TOF	TON	TOF
WOC 1							
1	0.5	CAN	10	2024	16	1608	
2	1.0	CAN	10	1036	12	1101	
3	2.5	CAN	11	422	12	421	31
4	5.0	CAN	12	199	13	230	16
5	1.0	CAN ^c	12	868	10	734	
6	2.5	CAN ^c	11	761	11	758	
7	5.0	CAN ^c	14	486	9	458	
8	1.0	NaIO_4			19	2192	14
9	2.5	NaIO_4			19	963	9
10	5.0	NaIO_4			14	482	7
11	10.0	NaIO_4			12	256	
WOC 2							
12	0.3	CAN ^b	53	2731	61	2937	
13	0.5	CAN ^b	112	1886	116	2325	
14	1.0	CAN ^b	101	855	95	945	
15	2.5	CAN ^b	73	400	66	378	22
16	5.0	CAN ^b	59	200	48	220	14
17	1.0	CAN ^c	54	2356	74	2430	
18	2.5	CAN ^c	69	782	88	990	
19	5.0	CAN ^c	59	363	76	463	
20	10.0	CAN ^c	34	175			
21	0.5	NaIO_4			6	1430	
22	1.0	NaIO_4			7	1779	
23	2.5	NaIO_4			5	783	1
24	5.0	NaIO_4			4	419	2

^aTON and TOF (in min^{-1}) evaluated by UV-Vis spectroscopy, manometry and Clark electrode; ^b [SO] = 5 mM; ^c [SO] = 10 mM.

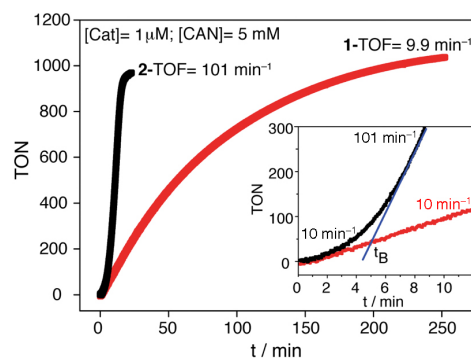


Figure 2. Time-conversion profile for WOCs from **1** and **2** measured by UV-Vis spectroscopy (CAN = 5mM; [Ir] = 1 μM ; pH 1 by HNO_3). The inset shows identical behavior for both catalysts initially, and remarkably higher activity for complex **2** compared to **1** after the bifurcation time t_B (note the absence of any significant induction time).

The time of bifurcation t_B was extracted from the interception of the slopes of the initial rate (at early t) and the linear

high rate for **2** as illustrated in the inset of Figure 2. Interestingly, t_B depends on the concentration of the catalyst but is independent of the CAN concentration, which is used in large excess (Figure 3). The furcation occurs later when $[\text{Ir}]$ is low, suggesting that the initially formed active species (Ir_A)—presumably similar for **1** and **2**—undergoes an associative transformation that is induced by the octyl groups, leading to a much more complex and active species (Ir_B) when CAN is used as sacrificial oxidant. Irrespective of the chemical nature of Ir_B , the combination of **2** and CAN results in 10 times higher TOFs than with **1** and CAN. For complex **2**, the activity depends on the concentration of both catalyst and CAN (Figure 4). For example, at 5 mM CAN concentration, a maximum TOF = 112 min^{-1} was observed at $[\text{Ir}] = 0.7 \mu\text{M}$, while at 10 mM CAN, the highest TOF = 74 min^{-1} was achieved at $[\text{Ir}] = 3.5 \mu\text{M}$. The dependence of the oxygen evolution rate on the iridium concentration is qualitatively similar at different CAN concentrations and reveals an optimum rather than a maximum in iridium concentration. This behavior might point to a steady state concentration of active species which has a maximum that is determined by both $[\text{Ir}]$ and $[\text{CAN}]$.

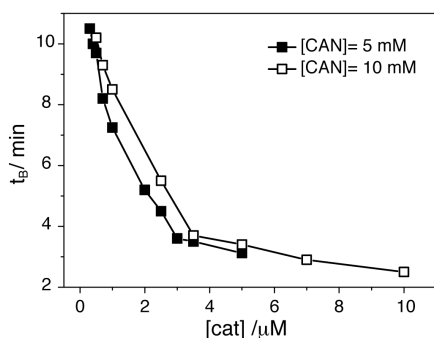


Figure 3. Dependence of bifurcation time t_B on concentration of **2** for two values of CAN concentration (determined by UV-Vis spectroscopy).

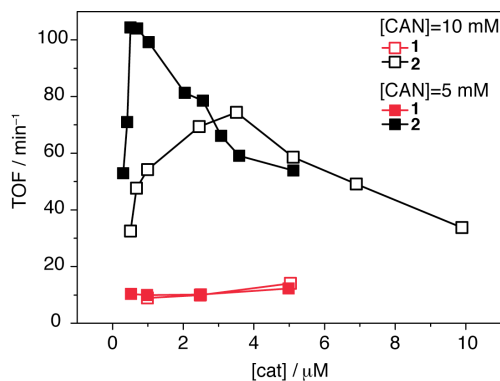


Figure 4. Different behavior of complexes **1** and **2**: while the activity of complex **1** is independent of catalyst concentration and activity, complex **2** reveals rate variability determined by the concentration of iridium and CAN (determined by UV-Vis spectroscopy).

The markedly higher activity of complex **2** with CAN appears to be related to an associative process, as indicated by the dependence of t_B on the iridium concentration (Figure 3). A plausible hypothesis for association involves the formation of micelles due to the amphiphilic character of complex **2** with long aliphatic substituents. Such micelles may organize the active iridium centers in close mutual proximity and may thus facilitate the usually rate-limiting O–O bond formation step through an I2M-type mechanism.^{18a–b}

In order to probe a potential associative process and the self-aggregation tendency of **1** and **2**, diffusion NMR experiments were performed. These measurements allow the self-diffusion translational coefficient (D_t) of a species in solution to be determined.¹⁹ Because D_t is related to the hydrodynamic radius, the dimension of molecular and supramolecular species can be accurately deduced. The average level of aggregation is readily disclosed by the aggregation number (N), defined as the ratio between the measured hydrodynamic volume (V_H) and that expected for the monomeric starting species (V_H^0).²⁰ Despite the presence of an octyl chain, **2** exhibits only a marginally higher self-aggregation tendency than **1** (Table 2). In D_2O , aggregation numbers were $N = 1.4$ and 1.8 for **1** (0.3 mM) and **2** (0.1 mM), respectively, suggesting for both compounds an equilibrium between a monomeric and dimeric species that is slightly more shifted towards the dimer for **2**, due presumably to enhanced hydrophobic interactions. In order to explore the self-aggregation tendency of **1** and **2** under conditions that are as relevant as possible to catalysis, titration experiments were performed with CAN (1 M DNO_3 , $\text{pD} = 1$) and NaIO_4 . A gradual oxidative transformation of the Cp^* ligand was detected, initiated by Cp^*-CH_3 to $\text{Cp}^*-\text{CH}_2\text{OH}$ oxidation,⁹ and ultimately leading to the complete disappearance of the Cp^* resonance from the ^1H NMR spectrum.^{10a} The oxidative transformation of Cp^* is essentially identical with CAN and NaIO_4 , though the process is much faster with CAN.²¹ ^1H diffusion NMR experiments with acquisition time up to 3 days were performed using 0.1–1.0 mM solutions of **1** and **2** in the presence of 20–30 equivalents of oxidant.¹⁷ Under these conditions, the phenyl and alkyl protons appeared as broad resonances, yet sufficiently intense for evaluating D_t . The deduced V_H values for **1** and **2** changed only little (Table 2) and gave aggregation numbers $N = 1.4$ and 1.7 (for **1** with CAN and NaIO_4 , respectively) and $N = 2.0$ (for **2** with either CAN or NaIO_4), when referenced to V_H^0 of the initial precursors. Larger aggregation numbers result when assuming that the Cp^* ligand completely transforms into acetic acid, formic acid and CO_2 and that a dimeric iridium species $[(\text{C},\text{N})\text{X}_2\text{Ir}(\mu^2\text{-X})_2\text{IrX}_2(\text{C},\text{N})]$ forms, analogous to Crabtree's proposal ($X = \text{oxo}, \text{hydroxo}$).²² The hydrodynamic volumes for these dimers derived from **1** and **2** were estimated to be 657 \AA^3 and 951 \AA^3 , respectively. These values agree very well with the measured V_H for the active species evolving from **1**, while the species originating from **2** unveils a

slightly higher aggregation tendency. Irrespective of the exact nature, the self-association propensity of **2** is not significantly different with either CAN or NaIO₄, thus suggesting that the SO is not directly involved in the associative process. Further support for the formation of small aggregates only was obtained from DLS experiments, which did not reveal any particles in the 3–500 nm hydrodynamic radius range.

Table 2. Oxidant-dependent hydrodynamic volume (V_H) and aggregation number (N) of complexes **1 and **2** from diffusion NMR spectroscopy.^a**

complex	oxidant	$V_H / \text{\AA}^3$	N
1	none	670	1.4
1	NaIO ₄	790	1.7
1	CAN	690	1.4
2	none	1080	1.8
2	NaIO ₄	1180	2.0
2	CAN	1214	2.0

^a Aggregation number N based on $V_H^0(\mathbf{1}) = 470 \text{ \AA}^3$ and $V_H^0(\mathbf{2}) = 600 \text{ \AA}^3$; see reference 19.

The general picture emerging from our results is consistent with the generation of several catalytically active species for both **1** and **2**, all having molecular nature, due to the oxidative transformation of Cp* with both CAN and NaIO₄. According to diffusion NMR measurements, it is reasonable to conclude that all species stemming from **2** have a slightly higher tendency to self-aggregate than analogues derived from **1**. The self-aggregation of one specific species derived from the oxidative transformation of **2** conceivably generates a catalyst with an extraordinarily high activity. Among the various potential reasons for the particular role of CAN, we speculate that oxidative transformation with NaIO₄ is unfavorably slow compared with catalytic turnover frequencies, while Cp* oxidation with CAN occurs readily to form the highly active aggregate. In such a model, the steady state concentration of the self-assembled species is finely tuned by CAN and catalyst concentrations thus rationalizing the delicate balance required for optimum rates (*cf* Figure 4).

In conclusion, a simple and remote modification in the ancillary carbene ligand of triazolylidene Ir(Cp*) complexes leads to an increase of water oxidation by one full order of magnitude and affords one of the highest oxygen evolution rates that has been recorded thus far for iridium-catalyzed water oxidation. The substantial rate enhancement is potentially induced by a specific aggregation process. Even though the incorporation of lipophilic elements into a catalyst for water oxidation appears highly counterintuitive, the introduction of long alkyl chains may become an essential feature when designing molecular water oxidation catalysts with exceptionally high activity, also when considering metal complexes other than those based on iridium.

ASSOCIATED CONTENT

Supporting Information. Synthetic procedures, chemical water oxidation details, NMR measurements, crystallographic details and DLS measurements. This material is available free of charge via the Internet at <http://pubs.acs.org>.

AUTHOR INFORMATION

Corresponding Author

alceo.macchioni@unipg.it
martin.albrecht@ucd.ie

Notes

The authors declare no competing financial interest.

ACKNOWLEDGMENT

This work was financially supported by SABIC, the European Research Council (CoG 615653), Science Foundation Ireland, and COST Action CM1205 (CARISMA).

REFERENCES

- (a) Alstrum-Acevedo, J. H.; Brennaman, M. K.; Meyer, T. J. *Inorg. Chem.* **2005**, *44*, 6802–6827. (b) Lewis, N. S.; Nocera, D. G. *Proc. Natl. Acad. Sci.* **2006**, *103*, 15729–15735. (c) Balzani, V.; Credi, A.; Venturi, M. *ChemSusChem* **2008**, *1*, 26–58. (d) Gust, D.; Moore, T. A.; Moore, A. L. *Acc. Chem. Res.* **2009**, *42*, 1890–1898. (e) McDaniel, N. D.; Bernhard, S. *Dalton Trans.* **2010**, *39*, 10021–10030. (f) Berardi, S.; Drouet, S.; Francàs, L.; Gimbert-Suriñach, C.; Guttentag, M.; Richmond, C.; Stoll, T.; Llobet, A. *Chem. Soc. Rev.* **2014**, *43*, 7501–7519.
- For leading and recent references, see: (a) Dau, H.; Limberg, C.; Reier, T.; Risch, M.; Roggan, S.; Strasser, P. *ChemCatChem* **2010**, *2*, 724–761. (b) Cao, R.; Lai, W.; Du, P. *Energy Environ. Sci.* **2012**, *5*, 8134–8157. (c) Liu, X.; Wang, F. *Coord. Chem. Rev.* **2012**, *256*, 1115–1136. (d) Hettler, D. G. H.; Reek, J. N. H. *Angew. Chem. Int. Ed.* **2012**, *51*, 9740–9747. (e) Wasylenko, D. J.; Palmer, R. D.; Berlinguette, C. P. *Chem. Commun.* **2013**, *49*, 218–227. (f) Kärkäs, M. D.; Verho, O.; Johnston, E. V.; Åkermark, B. *Chem. Rev.* **2014**, *114*, 11863–12001.
- For a recent example of a molecular catalyst immobilized onto a functional material see: Savini, A.; Bucci, A.; Nocchetti, M.; Viviani, R.; Idriss, H.; Macchioni, A. *ACS Catal.* **2015**, *5*, 264–271.
- Molecular Water Oxidation*, Llobet, A., Ed., Wiley-Interscience: New York, 2014.
- Duan, L.; Bozoglian, F.; Mandal, S.; Stewart, B.; Privalov, T.; Llobet, A.; Sun, L. *Nat. Chem.* **2012**, *4*, 418–423.
- Woods, J. A.; Bernhard, S.; Albrecht M. in: *Molecular Water Oxidation*, Llobet, A., Ed., Wiley-Interscience: New York, 2014; pp 113–133.
- McDaniel, N. D.; Coughlin, F. J.; Tinker, L. L.; Bernhard, S. *J. Am. Chem. Soc.* **2008**, *130*, 210–217.
- For selected examples, see: (a) Hull, J. F.; Balcells, D.; Blakemore, J. D. C.; Incarvito, D.; Eisenstein, O.; Brudvig, G. W.; Crabtree, R. H. *J. Am. Chem. Soc.* **2009**, *131*, 8730–8731. (b) Savini, A.; Bellachioma, G.; Ciancaleoni, G.; Zuccaccia, C.; Zuccaccia, D.; Macchioni, A. *Chem. Commun.* **2010**, *46*, 9218–9219. (c) Hettler, D. G. H.; Reek, J. N. H. *Chem. Commun.* **2011**, *47*, 2712–2714. (d) Marquet, N.; Gärtner, F.; Losse, S.; Pohl, M.-M.; Junge, H.; Beller, M. *ChemSusChem* **2011**, *4*, 1598–1600. (e) Bucci, A.; Savini, A.; Rocchigiani, L.; Zuccaccia, C.; Rizzato, S.; Albinati, A.; Llobet, A.; Macchioni, A. *Organometallics* **2012**, *31*, 8071–8074. (f) Wang, C.; Wang, J.-L.; Lin, W. *J. Am. Chem. Soc.* **2012**, *134*, 19895–19908. (g) Codolà, Z.; Cardoso, J. M. S.; Royo, B.; Costas, M.; Fillol, J. L. *Chem. Eur. J.* **2013**, *19*, 7203–7213. (h) DePasquale, J.; Nieto, I.; Reuther, L.E.; Herbst-Gervasoni, C. J.; Paul, J. J.; Mochalin, V.; Zeller, M.; Thomas, C.

M.; Addison, A. W.; Papish, E. T. *Inorg. Chem.* **2013**, *52*, 9175–9183. (i) Lewandowska-Andralojc, A.; Polyansky, D. E.; Wang, C.-H.; Wang, W.-H.; Y. Himeda, Fujita, E. *Phys. Chem. Chem. Phys.* **2014**, *16*, 11976–11987. (j) Savini, A.; Bucci, A.; Bellachioma, A.; Giancola, S.; Palomba, F.; Rocchigiani, L.; Rossi, A.; Suriani, A.; Zuccaccia, C.; Macchioni A. *J. Organomet. Chem.* **2014**, *771*, 24–32.

9) (a) Grotjahn, D. B.; Brown, D. B.; Martin, J. K.; Marelius, D. C.; Abadjian, M.-C.; Tran, H. N.; Kalyuzhny, G.; Vecchio, K. S.; Specht, Z. G.; Cortes-Llamas, S. A.; Miranda-Soto, V.; van Niekerk, C.; Moore, C. E.; Rheingold, A. L. *J. Am. Chem. Soc.* **2011**, *133*, 19024–19027. (b) Savini, A.; Belanzoni, P.; Bellachioma, G.; Zuccaccia, C.; Zuccaccia, D.; Macchioni, A. *Green Chem.* **2011**, *13*, 3360–3374. (c) Zuccaccia, C.; Bellachioma, G.; Bolaño, S.; Rocchigiani, L.; Savini, A.; Macchioni, A. *Eur. J. Inorg. Chem.* **2012**, 1462–1468.

10) (a) Zuccaccia, C.; Bellachioma, G.; Bortolini, O.; Bucci, A.; Savini, A.; Macchioni, A. *Chem. Eur. J.* **2014**, *20*, 3446–3456. (b) Savini, A.; Bucci, A.; Bellachioma, G.; Rocchigiani, L.; Zuccaccia, C.; Llobet, A.; Macchioni, A. *Eur. J. Inorg. Chem.* **2014**, 690–697.

11) (a) Joya, K.S.; Subbaiyan, N. K.; D'Souza, F.; de Groot, H. J. M. *Angew. Chem. Int. Ed.* **2012**, *51*, 9601–9605. (b) Diaz-Morales, O.; Hersbach, T. J. P.; Hetterscheid, D. G. H.; Reek, J. N. H.; Koper, M. T. M. *J. Am. Chem. Soc.* **2014**, *136*, 10432–10439.

12) (a) Thomsen, J. M.; Sheehan, S. W.; Hashmi, S. M.; Campos, J.; Hintermair, U.; Crabtree, R. H.; Brudvig, G. W. *J. Am. Chem. Soc.* **2014**, *136*, 13826–13834. (b) Savini, A.; Bellachioma, G.; Bolaño, S.; Rocchigiani, L.; Zuccaccia, C.; Zuccaccia, D.; Macchioni, A. *ChemSusChem* **2012**, *5*, 1415–1419.

13) (a) Lalrempuia, R.; McDaniel, N. D.; Müller-Bunz, H.; Bernhard, S. Albrecht, M. *Angew. Chem. Int. Ed.* **2010**, *49*, 9765–9768. (b) Petronilho, A. Rahman, M.; Woods, J. A.; Al-Sayyed, H.; Müller-Bunz, H.; Don, M. J. M.; Bernhard, S.; Albrecht, M. *Dalton Trans.* **2012**, *41*, 13074–13080. (c) Woods, J. A. Lalrempuia, R.; Petronilho, A.; McDaniel, N. D.; Müller-Bunz, H.; Albrecht, M.; Bernhard, S. *Energy Env. Sci.* **2014**, *7*, 2316–2328.

14) (a) Mathew, P.; Neels, A.; Albrecht, M. *J. Am. Chem. Soc.* **2008**, *130*, 13534–13535. (b) Guisado-Barrios, G.; Bouffard, J.; Donnadiou, B.; Bertrand, G. *Angew. Chem. Int. Ed.* **2010**, *49*, 4759–4762. (c) Crowley, J. D.; Lee, A.-L.; Kilpin, K. J. *Aust. J. Chem.* **2011**, *64*, 1118–1132. (d) Donnelly, K. F.; Petronilho, A.; Albrecht, M. *Chem. Commun.* **2013**, *49*, 1145–1159.

15) For a review on the properties of sacrificial oxidants for WO see: (a) Parent, A. R.; Crabtree, R. H.; Brudvig, G. W. *Chem. Soc. Rev.* **2013**, *42*, 2247–2252. For a more recent paper on IO_4^- as oxidant for WO see: (b) Hetterscheid, D. G. H.; Reek, J. N. H. *Eur. J. Inorg. Chem.* **2014**, 742–749.

16) Kwok, S. W.; Fotsing, J. R.; Fraser, R. J.; Rodionov, V. O.; Fokin, V. V. *Org. Lett.* **2010**, *12*, 4217–4219.

17) See supporting information for details.

18) (a) Romain, S.; Vigar, L.; Llobet, A. *Acc. Chem. Res.* **2009**, *42*, 1944–1953. (b) Petronilho, A.; Woods, J. A.; Bernhard, S.; Albrecht, M. *Eur. J. Inorg. Chem.* **2014**, 708–714.

19) Macchioni, A.; Ciancaleoni, G.; Zuccaccia, C.; Zuccaccia, D. *Chem Soc. Rev.* **2008**, *37*, 479–489.

20) V_{ii}^0 was derived by multiplying the van der Waals volume of the crystal structures of **1** and **2** by 1.3, see reference 19 for details.

21) No degradation of the triazolylidene ligand was noted under these conditions. Exposure of complex **2** to 40 equivalent of CAN in 1 M HNO_3 for 2 h, and subsequent extraction of organic residues with CH_2Cl_2 did not reveal any formation of octanol, octanal, or octanoic acid in the organic layer, even though such compounds would readily extract from acidic water into CH_2Cl_2 . Instead, only small traces of complex **2** were recovered. These experiments are in agreement with a robust ligand structure under these oxidizing and acidic conditions, and do not support oxidative C–N bond cleavage in the triazolylidene ligand.

22) Hintermair, U.; Sheehan, S. W.; Parent, A. R.; Ess, D. H.; Richens, D. T.; Vaccaro, P.H.; Brudvig, G. W.; Crabtree, R. H. *J. Am. Chem. Soc.* **2013**, *135*, 10837–10851.

